

RESEARCH LETTER

Open Access



Probing of meteor showers at Mars during the encounter of comet C/2013 A1: predictions for the arrival of MAVEN/Mangalyaan

Syed A Haider^{1*} and Bhavin M Pandya²

Abstract

We have estimated (1) production rates, (2) ion and electron densities of meteor ablation and (3) ionization for different masses and velocities of meteoroids when comet C/2013 A1 crossed the orbit of Mars on 19 October, 2014 at 18:27 UT. Meteor ablations of small masses $< 10^{-4}$ g have created a broad layer between altitude ~ 90 km and 110 km. The meteoroids of large masses $\geq 10^{-4}$ g are burnt at around 60–90 km well below the main ionization peak at altitude ~ 160 km produced in the nighttime by solar wind particle impact. The production rates and densities of 15 metallic ions (Mg^+ , Fe^+ , Si^+ , MgO^+ , FeO^+ , SiO^+ , $MgCO_2^+$, MgO_2^+ , $FeCO_2^+$, FeO_2^+ , $SiCO_2^+$, SiO_2^+ , MgN_2^+ , FeN_2^+ , and SiN_2^+) have been computed self-consistently between altitudes 50 km and 150 km. The twelve major peaks in the Ion Mass Spectra (IMS) are predicted by our model calculations. Our predicted ion and electron density profiles of metals provide benchmark values that can be observed by plasma probes onboard Mars Express (MEX), Mars Atmosphere and Volatile Evolution (MAVEN) and Mangalyaan.

Introduction

The comet C/2013 A1 was discovered on 3 January, 2013 at Siding Spring Observatory using Uppsala Southern Schmidt Telescope (<http://ssd.jpl.nasa.gov/sbdb.cgi>). It passed from the environment of Mars at minimum distance ~ 134000 km (equal to 0.00059 AU) on 19 October, 2014 at nighttime [1]. The closest approach of this comet with Mars is shown in Figure 1. Mangalyaan and MAVEN have been explored into Mars environment on 5 and 18 November, 2013 respectively. Both missions reached in the orbit of Mars during last week of September, 2014. The Neutral Gas Ion Mass Spectrometer (NGIMS) onboard MAVEN has sampled the compositions of Mars atmosphere and observed eight metals (i.e. Mg, Fe, Na, K, Mn, Ni, Cr and Zn) after the close encounter with C/2013A1 (mars.nasa.gov/comets/siding_spring). The Martian Exospheric Neutral Composition Analyzer (MENCA) onboard Mangalyaan should also measure the mass densities of cometary dust in the Martian environment (www.isro.org/mars/updates.aspx). Both missions do not carry radio occultation experiment. Therefore, they cannot

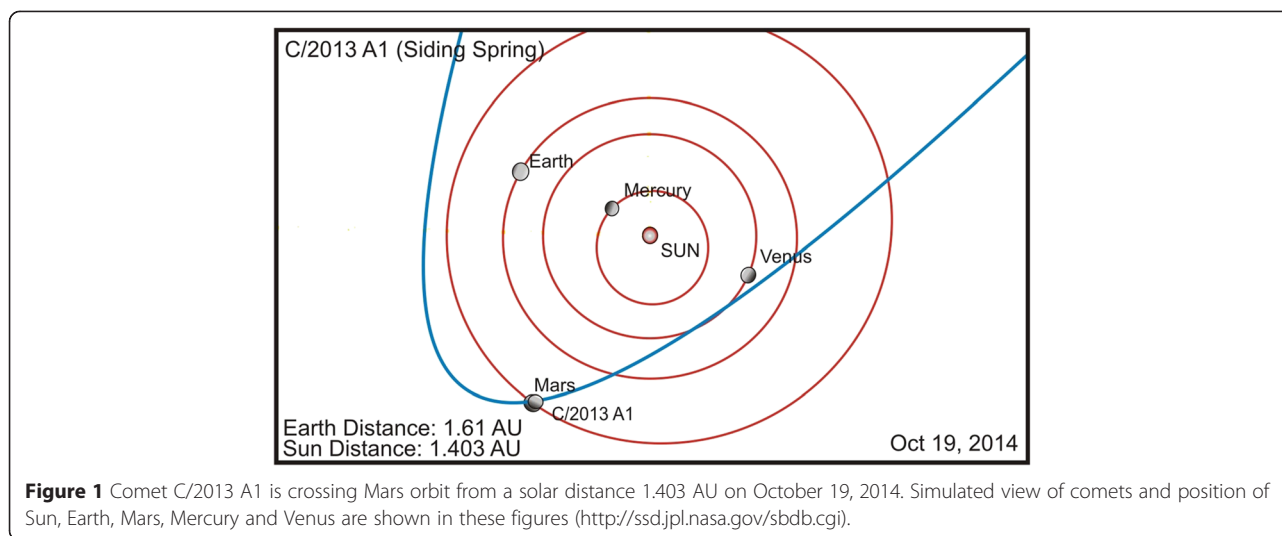
measure electron density profiles during this event. MEX is orbiting around Mars since April, 2004 (cf. [2]). It carries Mars Express radio science experiment (MaRS) which can observe electron density profiles in the atmosphere when the comet C/2013 A1 crossed the orbit of Mars. The Opportunity and Curiosity rovers landed on Mars on 25 January, 2004 and 6 August, 2013 respectively [3,4]. Their panoramic imaging cameras can also detect light of meteor bombardments in the environment of Mars during its encounter with this comet.

In this paper we have estimated production rates, ion and electron densities for meteor ionization of different masses and velocities of meteoroids at solar zenith angle (SZA) 110° . Our calculation suggests that two broad meteoric layers can be formed in the middle ionosphere during the encounter of the comet C/2013 A1 with the atmosphere of Mars. It is found that the meteor ablation of small masses $< 10^{-4}$ g would occur between altitude 90 km and 110 km where the free molecular path is several orders larger than the meteoroid size. This is known as micrometeoroids [5]. The meteoroids of large masses $\geq 10^{-4}$ g will penetrate deeper into the atmosphere and burn at altitude range 60 – 90 km. The predicted rate of ion formation and ion/electron density of

* Correspondence: haider@prl.res.in

¹Space and Atmospheric Sciences, Physical Research Laboratory, Navrangpura, Ahmedabad, India

Full list of author information is available at the end of the article



meteors of all masses increases with velocities of meteoroids. During the meteor showers the ion and electron density are increased by several orders of magnitude in the middle ionosphere of Mars.

Earlier measurements of meteoric layers on mars

The presence of meteoric layers at about 80 km was first reported in the night time from the observations made by Mars 4 and Mars 5 [6]. Later a meteor observing campaign was carried out by Panoramic camera (Pancam) onboard Mars Exploration Rover (MER) Spirit which detected two Martian showers on 18 November and 27 October 2005 when comet Halley and 2001/R1 LONEOS intersected the orbit of Mars from a close distance 0.067 AU and 0.001 AU, respectively. Domokos *et al.* [7] analyzed nighttime Pancam observations and estimated an upper limit of meteoroid flux $1.2 \times 10^{-19} \text{ cm}^{-2} \text{ s}^{-1}$ of mass larger than 4 g. Molina-Cuberos *et al.* [8] used micro sized meteoroid fluxes 10^{-19} to $10^{-17} \text{ cm}^{-2} \text{ s}^{-1}$ for masses $\sim 10^{-4}$ to 10^{-10} g and calculated maximum electron density $\sim 2 \times 10^4 \text{ cm}^{-3}$ and $3 \times 10^2 \text{ cm}^{-3}$ during the daytime and nighttime ionosphere of Mars at altitudes 85 km and 83 km respectively.

Mars Global Surveyor (MGS) has observed 5600 electron density profiles from radio science experiment during the period 24 December 1998 to 9 June 2005 [9-11]. Withers *et al.* [10] found meteoric layers in 71 out of these 5600 electron density profiles. They have reported mean peak electron density $(1.33 \pm 0.5) \times 10^4 \text{ cm}^{-3}$ in the meteoric layer at a mean altitude of 91.7 ± 4.8 km. Their analysis suggests that the characteristics of these meteoric layers vary with season, SZA and latitude. Later Pandya and Haider [12] analyzed 1500 MGS electron density profiles to study the physical characteristics of meteoric plasma layers over Mars during the period January-June 2005. They found that 65 electron density profiles out of these 1500 profiles were strongly perturbed with peak

densities $\sim (0.5-1.4) \times 10^4 \text{ cm}^{-3}$ at altitudes between 80 km and 105 km, presumably due to ionization of meteoric atoms. Using these profiles they examined TEC in the lower ionosphere of Mars and found that maximum values of TEC occurred on 21 January and 23 May 2005, when comets 2007 PL42 and 4015 Wilson-Harrington intersected the orbit of Mars from close distances of 1.49 AU and 1.17 AU, respectively. The TEC values were increased by a factor of 5-7 on these days. Pandya and Haider [12] associated this significant increase with the meteor showers that were produced when Mars crossed the dust stream left along the orbits of these comets. These meteor showers were detected on Mars at different locations and at different times. The meteor shower of 21 January 2005 was observed at SZA = 74.3° , latitude 77.7°N and longitude 197.2°E during summer season ($L_s = 147.4^\circ$). The meteor shower of 23 May 2005 was detected in the autumn season at $L_s = 216.2^\circ$, SZA = 84.9° , latitude = 65.1°N and longitude 20.2°E .

Since 2004 MaRS experiment has observed 557 electron density profiles in the daytime and nighttime ionosphere of Mars [13,14]. Patzold *et al.* [13] observed meteoroid layers in 8% electron density profiles (i.e. 10 of 120 electron density profiles) of MEX measurements during the daytime ionosphere. Recently Haider *et al.* [15] have identified meteoric layers in two electron density profiles of MEX observations carried out in the nighttime ionosphere also, one on 22 August and the other on 25 September, 2005.

Methods

Modeling and input parameters

Recently MEX has observed three ionization peaks in the nighttime ionosphere of Mars at altitudes ~ 80 -100 km, 120 km and 160 km, which were reproduced by model calculation due to impact of meteoroid, solar wind proton (≤ 10 KeV) and electron (≤ 1 KeV)

respectively (cf. [15]). We have used this model to calculate the production rates and electron densities at SZA 110° due to impact of micrometeoroids and meteoroids of different masses and velocities. These calculations are carried out between altitudes of 50 km and 150 km for meteor ablation that occurred on 19 October, 2014 during the encounter of comet/2013 A1 with Mars atmosphere. We have considered ablation of different meteoroids of masses $10^{-9} \leq m < 10^1$ g for fluxes $10^{-6} \leq f < 10^{-16}$ $\text{cm}^{-2} \text{s}^{-1}$ at interval of 10 g, where m and f are mass and flux of meteoroid particles respectively. The Figure 2 represents meteoroid spectrum obtained by measurements from Pioneers 8/11 HEOS and Pegasus satellites for large and small masses at 1.0 AU distance from the sun [16-18]. *Grun et al.* [19] have fitted this spectrum by interplanetary dust model. They have found that collision lifetime at 1.0 AU is small ($\sim 10^4$ years) for meteoroids of 10^{-4} to 1 g mass. For particles with masses $m \leq 10^{-5}$ g the lifetimes were considerably larger than the collision lifetimes. Upper limit of meteoroid flux at Mars is observed to be $< 10^{-15}$ $\text{cm}^{-2} \text{s}^{-1}$ from Spirit/MER cameras for mass larger than 4 g [7]. This value of meteoroid flux is also shown in Figure 2. We have taken meteoroid fluxes from Figure 2 in our model calculation. Drolshagen [20] have calculated meteor impact velocity distribution between 10 km/s to 30 km/s. Therefore, we have taken meteoroid velocities 10 km/s, 18 km/s and 30 km/s and performed the calculation at five small and six large size particles of masses 10^{-5} -to- 10^{-9} g and 10-to- 10^{-4} g respectively at 10 g interval. The large and small size particles are considered as meteoroids and micrometeoroids respectively. We have

scaled meteoroid fluxes of Figure 2 to Martian orbit according to $\phi_m = \phi_e \times R_m^{0.5}$ [21], where ϕ_e and ϕ_m are the particle fluxes of dust in the orbit of Earth and Mars respectively, R_m is the distance of Mars from the sun in AU. The solar wind electron-proton-hydrogen impact ionizations are not included in this model calculation because they are important above 120 km (cf. [15]).

Our chemical model depends on the temperature and density of the atmosphere. The nighttime temperature and density of gases CO_2 , N_2 , O_2 , O and CO are calculated by *Bougher et al.* [22] between altitude 100 km and 220 km for the period September to October 2014. They solved 3-D MTGCM (Mars Thermosphere General Circulation Model) to study the atmosphere of Mars at different local time, latitude, longitude and seasons. We have taken temperature and density from this model for 19 October, 2014 at altitude from 100 km to 150 km. Between 50 km and 100 km, the temperature and density of *Haider et al.* [15] are used after scaling them for 19 October, 2014. The equations of motion, ablation and energy are solved [8, 15] to calculate the ion production rates due to impact of meteoroids with different masses in the nighttime ionosphere of Mars. We have assumed cometary meteoroids which are composed of 61.7% oxygen, 24.2% silicon, 8.2% magnesium, and 5.9% iron in atoms of element to the total [23]. The ions Fe^+ , Mg^+ and Si^+ are produced due to meteor ablation in the nighttime ionosphere. The minimum velocities of Fe^+ , Mg^+ and Si^+ are taken 9.4, 11.1 and 11 km/s, respectively for the calculation of ionization probabilities. The rate coefficients of 57 chemical reactions given by *Haider et al.* [15] have been used to calculate electron density of metals. Using this chemical

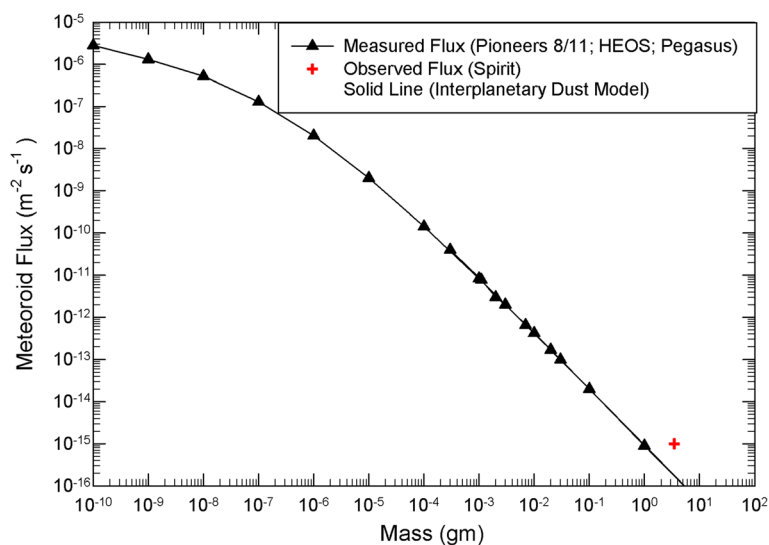


Figure 2 Meteoroids fluxes observed by Pioneers 8 and 11, HEOS, and Pegasus satellites at 1.0 AU. These fluxes are scaled to Mars orbit at 1.5 AU. Plus (+) shows upper limit of meteoroid flux measured by Opportunity/MER rovers on Mars [7]. Solid line represents Interplanetary Dust Model of *Grun et al.* [19].

scheme we have predicted IMS and electron density in the nighttime ionosphere for different masses and velocities of meteoroids.

We have solved continuity coupled equations under steady state condition to predict IMS spectra. In this calculation transport of ions is neglected because transport time is several orders of magnitude higher than the chemical lifetime. In this model densities of each ion species, n_i^+ , and electron, n_e , are calculated from the continuity equation and the charge neutrality condition using $P_i - l_i n_i^+ = 0$ and

$n_e - \sum n_i^+ = 0$, where P_i is the production rate by meteoroids/micrometeoroids and ion molecule reactions, and l_i is the specific loss due to ion-molecule reactions and recombination with electrons. We have also investigated densities of metallic clusters due to termolecular associations of metallic ions with neutral molecules. It should be noted that direct meteoric ionization is the only ionization source considered here. The ionization by solar radiation or photoelectrons at the peak altitude of the meteoroid/micrometeoroid ablation is low and its influence on the

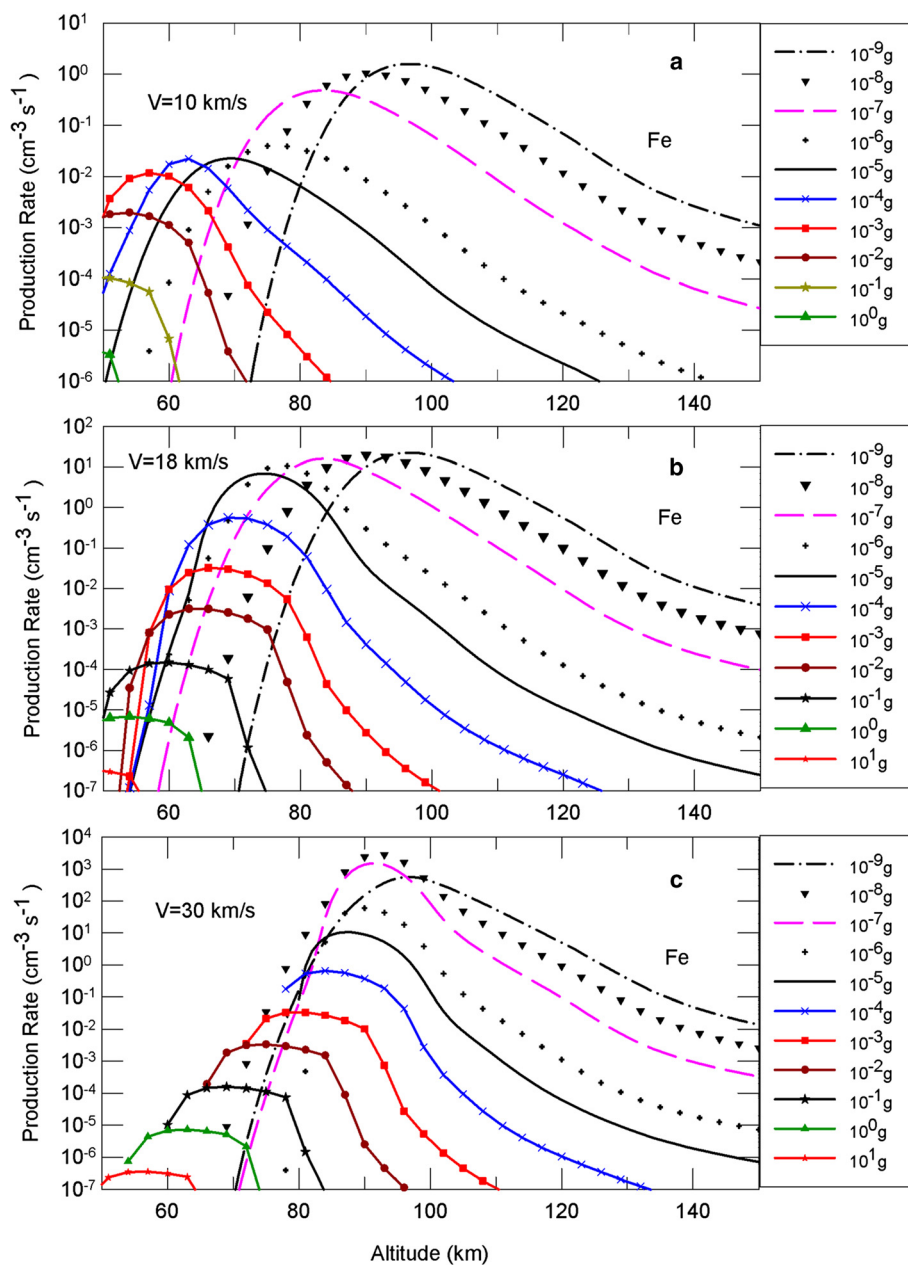


Figure 3 The estimated production rates of Fe in the Martian ionosphere at SZA 110° for different masses of meteoroids incoming at velocities 10 km/s (a), 18 km/s (b) and 30 km/s (c), when comet C/2013 A1 crossed the orbit of Mars on 19 October, 2014.

concentration of electrons and metallic ions is approximately negligible.

Results and discussion

In Figure 3a-c we have plotted production rates of Fe for different masses of meteoroids at velocities 10 km/s, 18 km/s and 30 km/s respectively. The production rates of Mg and Si are not plotted in Figure 3a-c because their values are similar to Fe. The productions of Fe are increasing with decreasing masses because meteoroid flux

is inversely proportional to mass of the metals [19]. The meteoroids of large masses penetrate deep into the atmosphere and were burnt at altitude range 60–90 km. The ablation of micrometeoroids takes place at altitude ~90–110 km where the free molecular path is by several orders larger than the meteoroid size. The maximum and minimum production rates of Fe are estimated to be $10^3 \text{ cm}^{-3} \text{ s}^{-1}$ and $5 \times 10^{-7} \text{ cm}^{-3} \text{ s}^{-1}$ due to impact velocity of 30 km/s. The production rates are decreasing with decreasing velocity of the particles because the flux

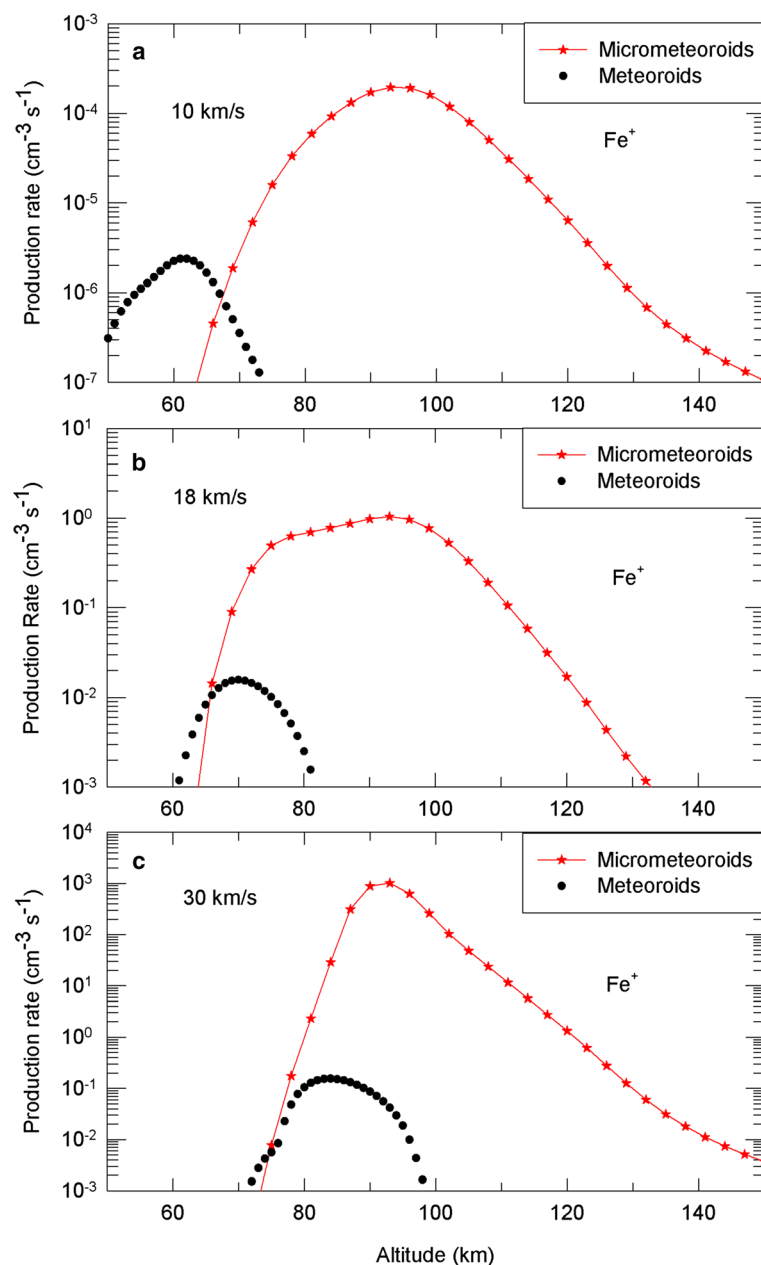


Figure 4 The estimated production rates of Fe^+ in the Martian ionosphere at SZA 110° for micrometeoroids and meteoroids incoming at velocities 10 km/s (a), 18 km/s (b) and 30 km/s (c), when comet C/2013 A1 crossed the orbit of Mars on 19 October, 2014.

is decreasing with the velocity. Figure 4a-c represent the ion production rates of Fe^+ due to ablation of micrometeoroids and meteoroids at velocities 10 km/s, 18 km/s and 30 km/s, integrated over masses 10^{-5} - 10^{-9} g and 10 - 10^{-4} g respectively. The production of Fe^+ ions by micrometeoroids is 2–3 orders of magnitude larger than the one due to meteoroids. We have estimated densities of 15 metallic ions Mg^+ , Fe^+ , Si^+ , MgO^+ , MgCO_2^+ , MgO_2^+ , MgN_2^+ , FeO^+ , FeO_2^+ , FeN_2^+ , FeCO_2^+ , SiO^+ , SiCO_2^+ , SiN_2^+ , and SiO_2^+ in the nighttime ionosphere of Mars. The electron density of meteoric layer is obtained from the sum

of the densities of all metallic ions of micrometeoroids and meteoroids. In Figure 5a-c we have plotted electron densities due to ablation of meteoroids and micrometeoroids at velocities 10 km/s, 18 km/s and 30 km/s respectively. The calculated peak heights and peak electron densities are compared in Table 1.

Recently, radio occultation experiment onboard MGS and MEX has observed meteoric plasma layers in the daytime and nighttime ionosphere of Mars at altitude range 80–100 km with peak electron density $\sim 10^3$ - 10^4 cm^{-3} [cf. [13-15]]. The density of meteoric layers

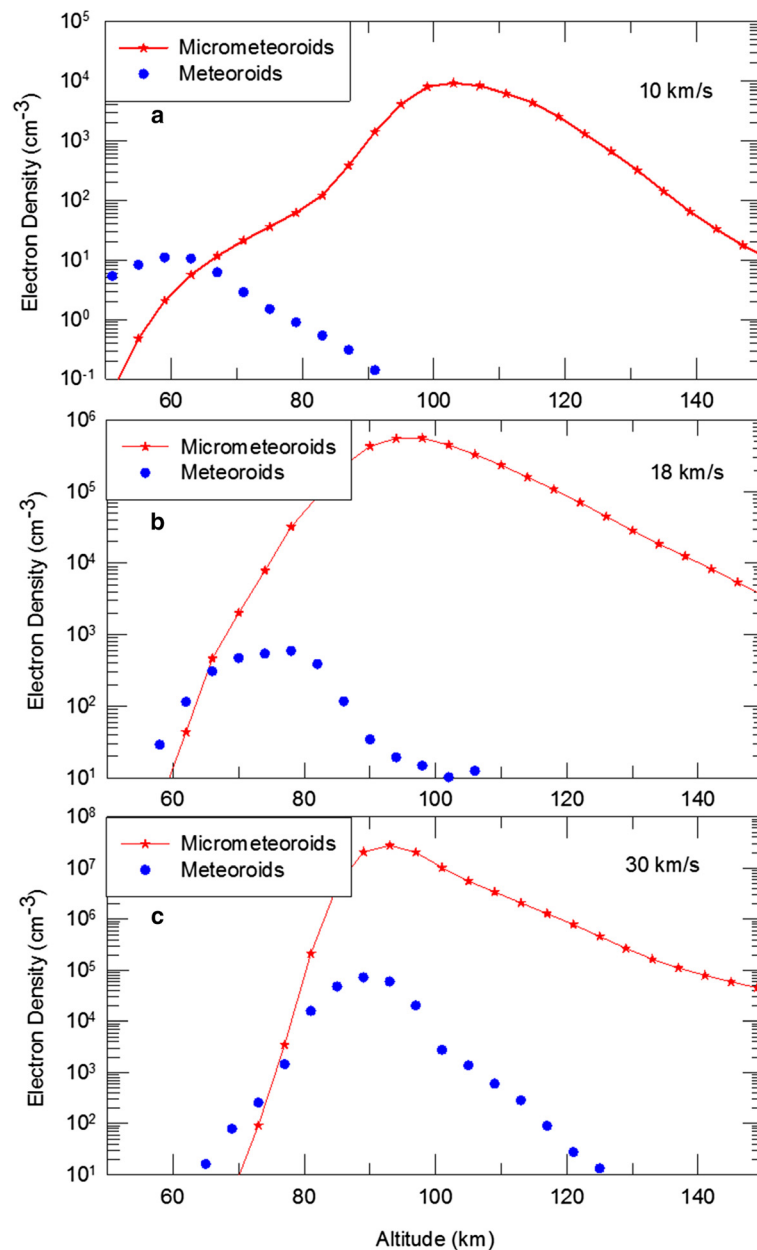


Figure 5 The predicted electron densities in the Martian ionosphere at SZA 110° for micrometeoroids and meteoroids incoming at velocities 10 km/s (a), 18 km/s (b) and 30 km/s (c), when comet C/2013 A1 crossed the orbit of Mars on 19 October, 2014.

Table 1 Peak height and peak electron densities due to micrometeoroids and meteoroids ablation at different velocities

Source	Velocity 10 km/s		Velocity 18 km/s		Velocity 30 km/s	
	Peak height (km)	Peak electron density(cm^{-3})	Peak height (km)	Peak electron density(cm^{-3})	Peak height (km)	Peak electron density(cm^{-3})
Micrometeoroids	105	$\sim 1.0 \times 10^4$	95	$\sim 3.5 \times 10^5$	90	$\sim 3.0 \times 10^7$
Meteoroids	60	$\sim 1.0 \times 10^1$	75	$\sim 6.0 \times 10^2$	90	$\sim 5.0 \times 10^4$

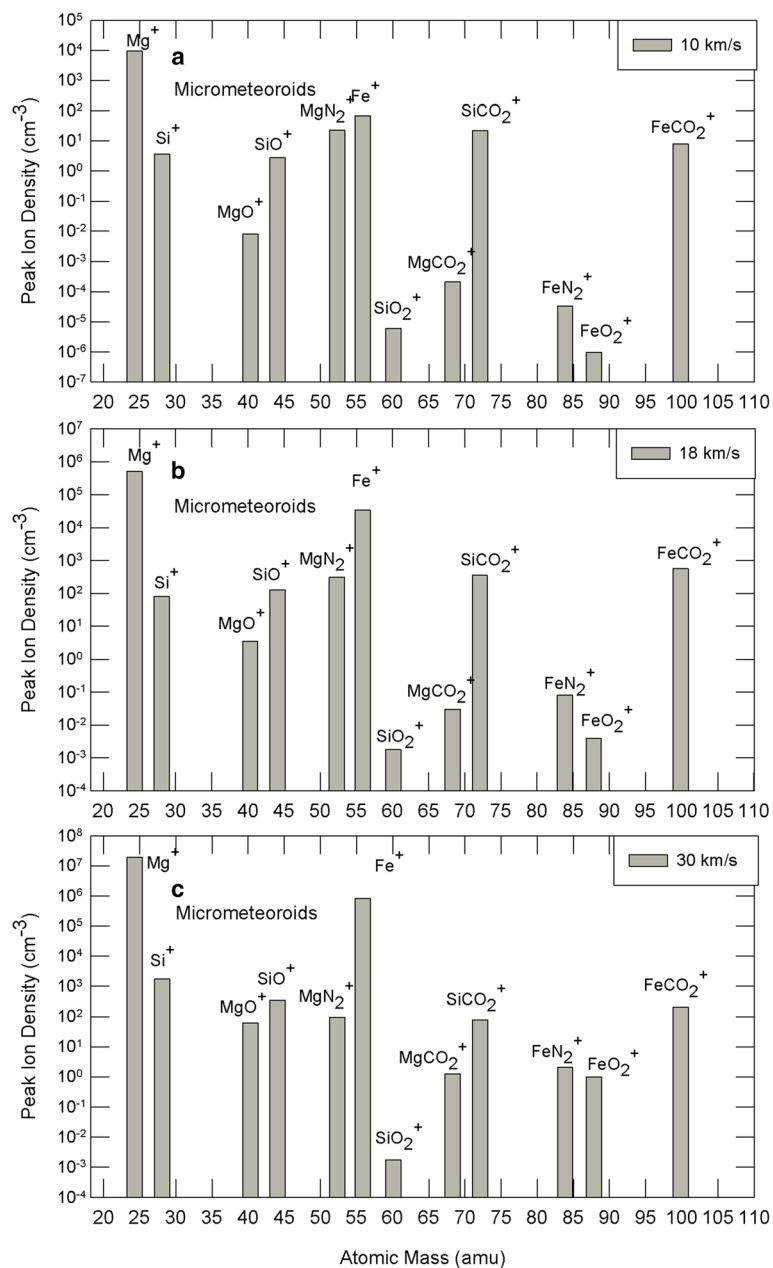


Figure 6 The predicted peak ion mass densities at SZA 110° for micrometeoroids incoming at velocities 10 km/s (a), 18 km/s (b) and 30 km/s (c), when comet C/2013 A1 crossed the orbit of Mars on 19 October, 2014.

can change with the intensity of meteor showers. We report that the predicted peak electron densities due to incoming micrometeoroids of velocities 18 km/s and 30 km/s are larger than MGS/MEX measurements by $\sim 2-3$ orders of magnitude. This suggests that the intensity of proposed meteor showers would be significantly large on 19 October, 2014 due to ablation of micrometeoroids of high velocity. Thus, high speed micrometeoroids will produce bright showers in the atmosphere of Mars. The calculated peak electron densities for incoming meteoroids of velocities

10 km/s and 18 km/s are lower than MGS/MEX measurements by $\sim 2-3$ orders of magnitude. The maximum electron densities predicted due to ablation of micrometeoroids and meteoroids of velocities 10 km/s and 30 km/s respectively are comparable in magnitude with these measurements.

Figures 6a-c and 7a-c represent the peak ion density spectra of fifteen masses between 24 and 100 amu due to ablation of micrometeoroids and meteoroids respectively at velocities 10 km/s, 18 km/s and 30 km/s. The

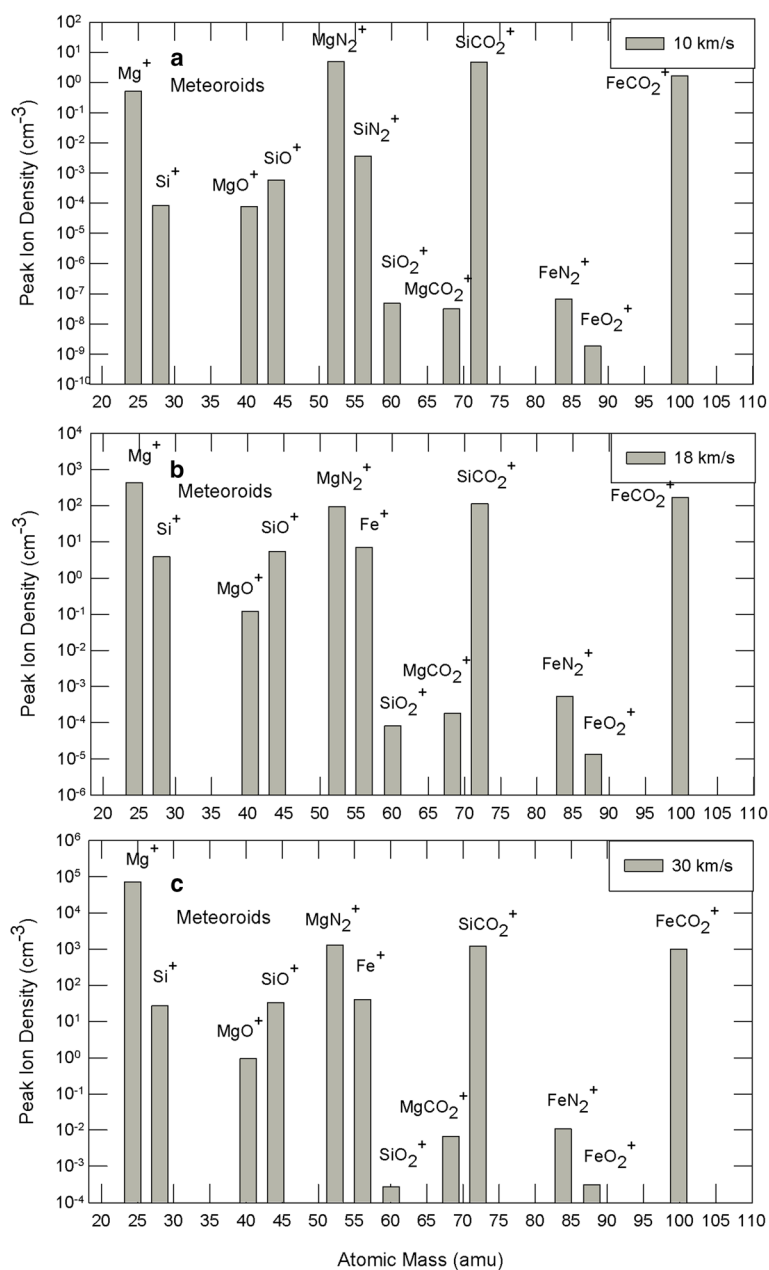


Figure 7 The predicted peak ion mass densities at SZA 110° for meteoroids incoming at velocities 10 km/s (a), 18 km/s (b) and 30 km/s (c), when comet C/2013 A1 crossed the orbit of Mars on 19 October, 2014.

density of each ion strongly depends on the incoming velocities and the peak ion densities are increasing with the impact velocities of cometary meteoroids and micrometeoroids. The mass of ions FeO^+ and MgO_2^+ / SiN_2^+ are close to the masses of SiCO_2^+ and Fe^+ respectively. Therefore, the mass densities of MgO_2^+ , SiN_2^+ and FeO^+ in IMS spectra cannot be separated. The mass densities of these ions are significantly lower than the mass densities of ions SiCO_2^+ and Fe^+ . The two most abundant ions Mg^+ and Fe^+ are produced due to micrometeoroids ablation at altitude > 90 km. At height < 90 km, twelve ions Fe^+ , Mg^+ , Si^+ , MgO^+ , SiO^+ , MgN_2^+ , SiO_2^+ , MgCO_2^+ , FeO^+ , FeN_2^+ , FeO_2^+ and FeCO_2^+ are produced due to meteoroids and micrometeoroids ablation.

Initially ions Mg^+ , Fe^+ and Si^+ are produced by direct meteoric ionization. The major cluster ions FeCO_2^+ and SiCO_2^+ are produced due to associations of Fe^+ and Si^+ with CO_2 by three body reactions. The other major cluster ion MgN_2^+ is also produced by three body reaction due to attachment of Mg^+ with N_2 . These cluster ions were lost by dissociative recombination reactions. The ions FeCO_2^+ and SiCO_2^+ are also produced from termolecular associations of Fe^+ and Si^+ with CO_2 respectively at the rate coefficient $1.0 \times 10^{-30} \text{ cm}^6 \text{ s}^{-1}$ [24]. The ions MgCO_2^+ , MgO_2^+ and MgN_2^+ are formed due to associations of CO_2 , O_2 , and N_2 with Mg^+ at rate constants 1.0×10^{-30} , $9.0 \times 10^{-30}(200/T)$ and $1.0 \times 10^{-30} \text{ cm}^6 \text{ s}^{-1}$ respectively [25-27]. The dissociative recombination rate coefficients of clusters were estimated to be $\sim 10^7 \text{ cm}^3 \text{ s}^{-1}$ [24,27,28], which is four orders of magnitude higher than the metallic ion recombination coefficient $\sim 10^{-12} \text{ cm}^3 \text{ s}^{-1}$ [cf. [24,29]]. The ions FeO^+ , SiO^+ and MgO^+ are formed due to loss of Fe^+ , Si^+ and Mg^+ with O_3 respectively. The densities of FeO^+ , SiO^+ and MgO^+ are lower than the densities of FeCO_2^+ , SiCO_2^+ and MgCO_2^+ respectively because the densities of O_3 is lower than CO_2 . In the meteoric layer of earth's ionosphere, termolecular reactions of metallic ions with oxygen followed by molecular dissociative recombination are very efficient processes. In the Mars atmosphere the concentration of oxygen is not high enough to decrease the concentration of metal ions through this reaction.

The ions Fe^+ , Si^+ and Mg^+ are also lost with O_2 by three body reactions, which produce less MgO_2^+ , FeO_2^+ and SiO_2^+ respectively because the density of O_2 is lower than CO_2 . Table 2 shows possible ion species that contribute to different peaks in IMS spectra from 24 to 100 amu. First, second, third, fourth, and fifth peaks at 24, 28, 40, 44 and 52 amu are contributed by Mg^+ , Si^+ , MgO^+ , SiO^+ and MgN_2^+ respectively. The ions for sixth peak at 56 amu are responsible for Fe^+ , SiN_2^+ and MgO_2^+ . At this channel Fe^+ is the major ion in the vicinity of the ionization peak. The seventh and eighth peaks are produced due to ions SiO_2^+ and MgCO_2^+ at

Table 2 Ion masses corresponding to ≤ 100 amu

Mass	Ions
24	Mg^+
28	Si^+
40	MgO^+
44	SiO^+
52	MgN_2^+
56	Fe^+ , MgO_2^+ , SiN_2^+
60	SiO_2^+
68	MgCO_2^+
72	FeO^+ , SiCO_2^+
84	FeN_2^+
88	FeO_2^+
100	FeCO_2^+

60 amu and 68 amu respectively. The ninth peak at 72 amu contains FeO^+ and SiCO_2^+ ions. The tenth, eleventh and twelve peaks are contributed by FeN_2^+ , FeO_2^+ and FeCO_2^+ at 84 amu, 88 amu and 100 amu respectively.

Figures 8a-c and 9a-c represent the peak height spectra of fifteen ions between 24 and 100 amu due to ablation of micrometeoroids and meteoroids of velocities 10 km/s, 18 km/s and 30 km/s respectively. At altitudes between 60–70 km and 70–80 km, the electron densities are mainly controlled by metallic ions Fe^+ , Si^+ and Mg^+ due to impact of meteoroids of velocities 10 km/s and 18 km/s respectively. The major ion Mg^+ is calculated between altitude 80–90 km due to ablation of meteoroids of velocity 30 km/s. The most abundant ions Fe^+ and Mg^+ are produced between altitudes 100 to 120 km due to ablation of micrometeoroids of velocity 10 km/s. The electron density between altitudes 90 to 100 km is produced from three major ions viz., Mg^+ , Fe^+ and FeO_2^+ due to impact of micrometeoroids of velocity 18 km/s. The maximum densities of nine ions (viz., Mg^+ , Si^+ , SiO^+ , Fe^+ , SiO_2^+ , MgCO_2^+ , FeO^+ , FeO_2^+ and FeCO_2^+) are calculated at altitude ~ 90 km due to ablation of micrometeoroids of velocity 30 km/s.

Uncertainty in the model

Our model depends on the neutral density, temperature, meteoroid flux and various chemical reactions. The neutral density and temperature are taken from *Bougher et al.* [22] for 19 October, 2014, when comet C/2013 A1 crossed the orbit of Mars. The meteoroid fluxes are not measured in the orbit of Mars. We do not know how much meteoroid flux will precipitate in the Martian ionosphere during ablation on 19 October, 2014. We have taken meteoroid fluxes from the measurements made by Pioneers 8/11 and Helios satellites in the orbit of earth with their experimental uncertainties of 15-20% [19].

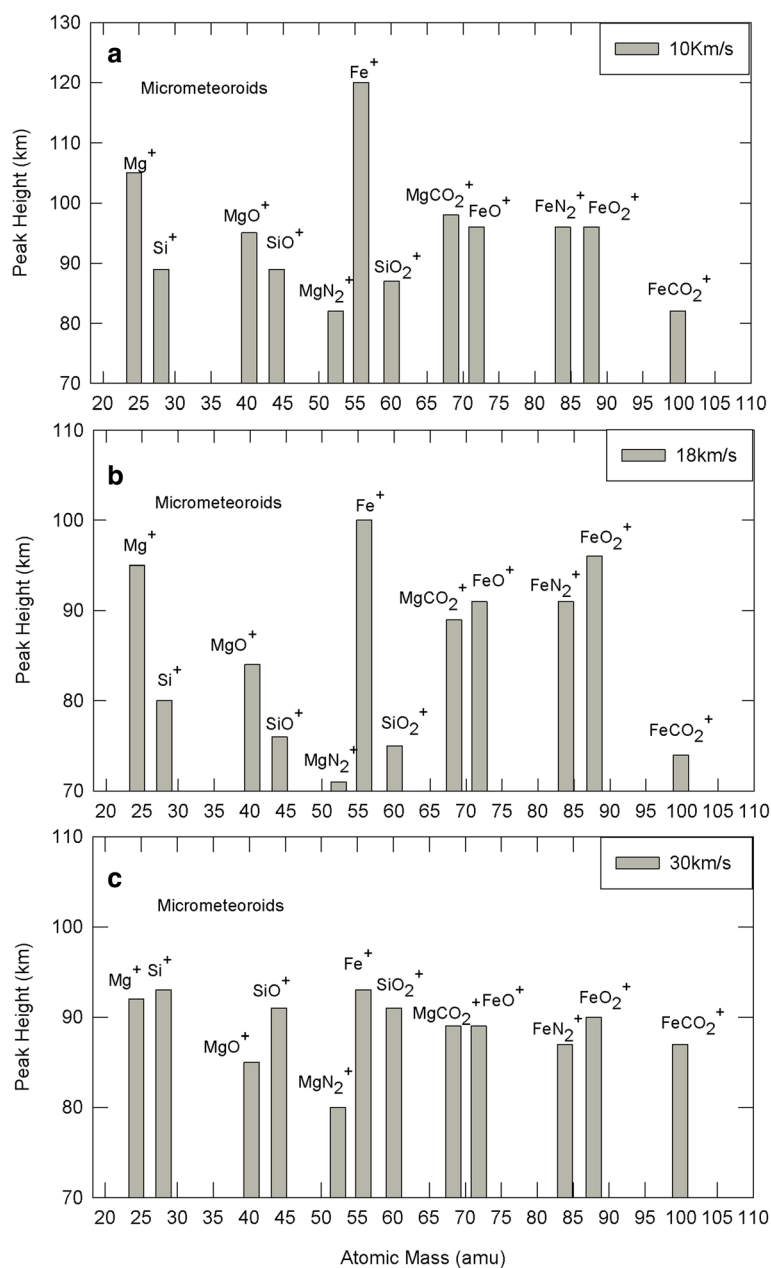


Figure 8 The predicted peak heights of metallic ion densities at SZA 110° for micrometeoroids incoming at velocities 10 km/s (a), 18 km/s (b) and 30 km/s (c), when comet C/2013 A1 crossed the orbit of Mars on 19 October, 2014.

These fluxes were scaled to Mars orbit. Some changes ~ 5–8% are expected in the ion and electron density due to this uncertainty in the model. However, scaled spectra of meteoroids are in good agreement with the upper limit of meteoroid flux measured by MER cameras for mass larger than 4 g at Mars. The present chemical model is developed by a sequence of algebraic expressions, which obtains solutions after sufficient iterations for ion and electron density. Transport effect of ions and electrons are omitted in this model because this effect is appreciable

above 200 km only. We note that above uncertainties are not very large.

Constraints on the meteor measurements from MAVEN and mangalyaan

Hubble Space Telescope observations indicated that the bulk of grains produced by comet C/2013 A1 will miss Mars. Only few percent of grains of higher velocities will reach Mars, peaking approximately 90–100 minutes after the close approach [30]. Later *Tricarico et al.* [31]

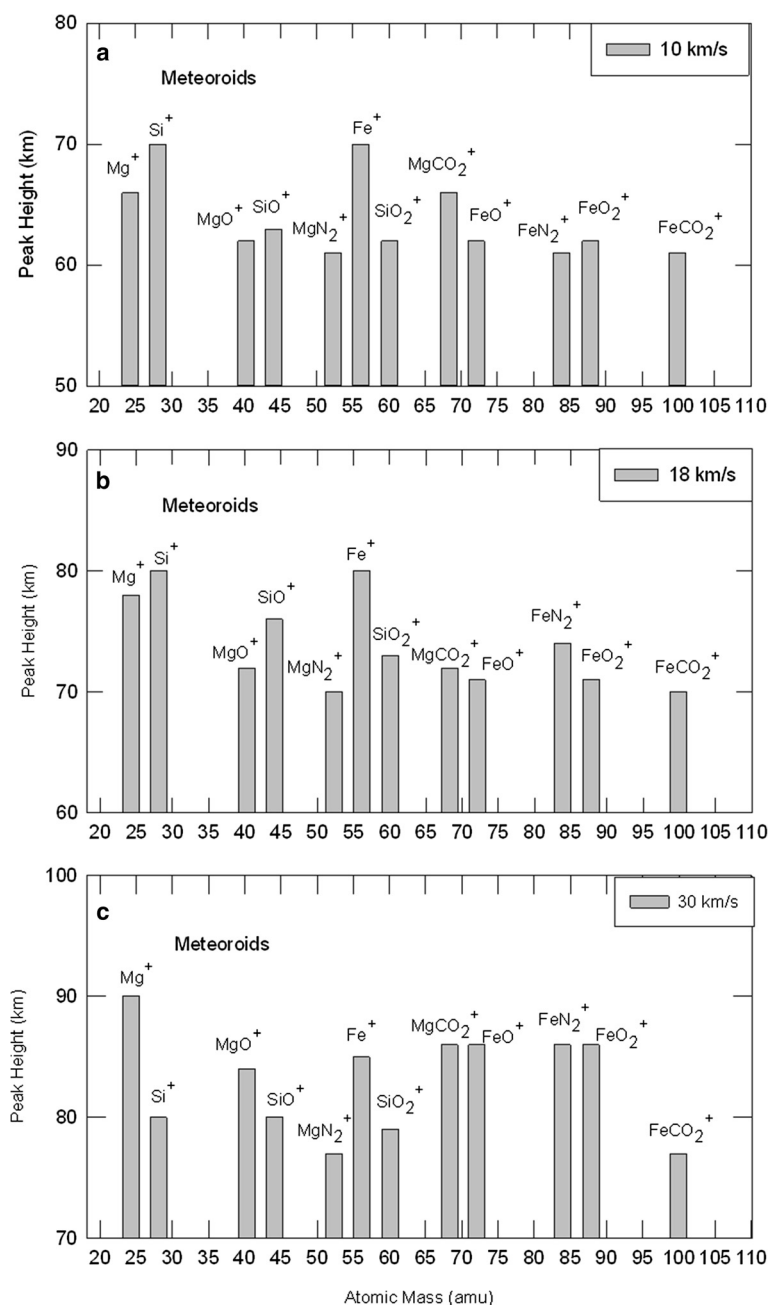


Figure 9 The predicted peak heights of metallic ion densities at SZA 110° for meteoroids incoming at velocities 10 km/s (a), 18 km/s (b) and 30 km/s (c), when comet C/2013 A1 crossed the orbit of Mars on 19 October, 2014.

confirmed that younger grains of sub millimeter to several millimeters can reach Mars at higher velocities. Based on model results of Kelley *et al.* [32] MAVEN, MEX and Mangalyaan were impacted by large dust grains and Mars received as many as $\sim 10^7$ grains (100 kg of total dust). The radio occultation experiment onboard MGS and MEX have observed meteoric plasma layers in most of the electron density profiles during daytime and nighttime ionosphere of Mars [cf. [2,11,15]]. MGS has now stopped

working since 2 November, 2006, but MEX is orbiting around Mars. However, MEX could not measure meteor electron density from this experiment on 19 October, 2014 during the encounters of comet C/2013 A1 with the atmosphere of Mars.

MAVEN and Mangalyaan are performing measurements from a highly elliptical orbit with a minimum height at about 150 km and 372 km respectively (www.isro.org/mars/updates.aspx; www.nasa.gov/mission_pages/maven/

main/). These missions did not carry radio occultation experiment, which can measure complete electron density profiles above 50 km. MAVEN carries Langmuir probe and ion/neutral mass spectrometer experiments. Mangalyaan also carries a mass spectrometer. Both experiments can measure plasma density in the upper atmosphere and exosphere of Mars. We have estimated meteoric ion and electron densities between altitude 50 km and 150 km for 19 October, 2014 due to intersection of comet C/2013 A1 with the atmosphere of Mars. The mass spectrometer onboard MAVEN is designed to measure ion concentrations as low as 0.1 cm^{-3} (www.nasa.gov/mission_pages/maven/main/). Using this instrument the meteor density is investigated for eight ions (i.e. Mg, Fe, Na, K, Mn, Ni, Cr and Zn) between masses 24 and 100 amu. Mangalyaan also carries a high resolution color camera operating in the visible range ($0.4 \mu\text{--}0.7 \mu$). This camera is measuring high quality visible images of Mars and its environments. The velocity of Mangalyaan at perigee ($\sim 372 \text{ km}$) is about 4 km/s where as it is less than 10 m/s at apogee ($\sim 80000 \text{ km}$) (www.isro.org/mars/updates.aspx). Thus, this mission allows imaging of localized scenes at higher spatial resolution as well as provides a synoptic view of the full globe during its elliptical orbit. Therefore, the light of meteor bombardments during occurrence of meteor shower on 19 October, 2014 can be detected from this color camera. The analysis of this data is under progress.

Conclusion

We have predicted two broad meteoric layers in the nighttime ionosphere of Mars at altitude range 90–110 km and 60–90 km due to ablation of micrometeoroids and meteoroids respectively, when comet C/2013 A1 crossed the orbit of Mars on 19 October, 2014. The mass densities of 15 metallic ions are also predicted in the vicinity of ionization peaks. These ions are produced by direct meteoric ionization and lost by dissociative recombination. The production rates are calculated using the equations of motion, ablation, and energy. The ion mass densities are estimated by coupled continuity equations controlled by steady state condition. The magnitude of the meteoric layers depends on the concentration of metals and incoming velocities, viz., 10 km/s , 18 km/s and 30 km/s of meteoroids and micrometeoroids. We have obtained that the concentrations of ions and electron strongly depend on the variations of the incoming velocities. It is also found that ion and electron densities can be increased by several orders of magnitude in the middle ionosphere of Mars during the meteor showers. Our estimated results can be confirmed in future by plasma probes onboard MAVEN and Mangalyaan.

Competing interests

The authors declare that they have no competing interest. We are exempt from paying article processing charges. We do not hold stock or shares in any organizations that may gain or lose financially from publication of this manuscript. We are not applying for any patents. There are no financial competing interests.

Authors' contributions

SAH has proposed the idea of meteoroid and micrometeoroid ablations on Mars. He has drafted, interpreted and analyzed the model results to prepare this manuscript. He has also presented this paper in AOGS 2014 meeting held in Sapporo, Japan. BMP has developed a model calculation of ion and electron densities caused by meteoroid/micrometeoroid ablations at different impact velocities in the atmosphere when comet C/2013 A1 will interact with Mars. Both authors read and approved the final manuscript.

Acknowledgement

Authors are thankful to MAVEN and Mangalyaan team for the discussion on Mars-comet tail intersection on 19 October, 2014 when meteor shower events can be detected by these missions. We also thank S.W. Bougher (email: bougher@umich.edu) for providing us density and temperature data obtained from Mars Thermosphere General Circulation Model (MTGCM) of Mars atmosphere for the month of October, 2014.

Author details

¹Space and Atmospheric Sciences, Physical Research Laboratory, Navrangpura, Ahmedabad, India. ²Permanent Address: Physics Department, C.U. Shah College, Ahmedabad, India.

Received: 24 September 2014 Accepted: 17 April 2015

Published online: 17 June 2015

References

- Farnocchia D, Chesley SR, Chodas PW, Tricarico P, Kelley MSP, Farnham TL (2014) Trajectory analysis for the nucleus and dust of comets C/2013 A1 (Siding Spring). *Astrophys J* 790:114
- Haider SA, Mahajan KK, Kallio E (2011) Mars ionosphere: A review of experimental results and modeling studies. *Rev Geophys* 49:37, doi: 10.1029/2011RG000357
- Arvidson RE, Ashley JW, Bell JF III, Chojnacki M, Cohen J, Economou TE, Farrand WH, Fergason R, Fleischer I, Geissler P, Gellert R, Golombek MP, Grotzinger JP, Guinness EA, Haberle RM, Herkenhoff KE, Herman JA, Iagnemma KD, Jolliff BL, Johnson JR, Klingelhöfer G, Knoll AH, Knudson AT, Li R, McLennan SM, Mittlefehldt DW, Morris RV, Parker TJ, Rice MS, Schröder C et al (2011) Opportunity Mars rover mission: Overview and selected results from Purgatory ripple to traverses to Endeavour crater. *J Geophys Res* 116:E00F15, Doi: 10.1029/2010JE003746
- Mahaffy PR, Webster CR, Atreya SK, Franz H, Wong M, Conrad PG, Harpold D, Jones JJ, Leshin LA, Manning H, Owen T, Pepin RO, Squyres S, Trainer M, MSL Science Team (2013) Abundance and isotopic composition of gases in the Martian atmosphere from the Curiosity Rover. *Science* 341(6143): 236–266, doi: 10.1126/science.1237966
- Love SG, Brownlee DE (1993) A direct measurement of the terrestrial mass accretion rate of cosmic dust. *Science* 262(5133):550–553
- Savich NA, Samovol VA (1976) The nighttime ionosphere of Mars from Mars 4 and Mars 5 dual frequency radio occultation measurements. *Space Res* XVI:1009–1010
- Domokos A, Bell JF, Brown P, Lemmon MT, Suggs R, Vaubaillon J, Cook W (2007) Measurement of the meteoroid flux at Mars. *Icarus* 191:141–150
- Molina-Cuberos GJ, Wittasse O, Lebreton J-P, Rodrigo R, Lopez-Moreno JJ (2003) Meteoric ions in the atmosphere of Mars. *Planet Space Sci* 51:239–249
- Withers P, Mendillo M (2005) Response of peak electron densities in the Martian ionosphere to day-to-day changes in solar flux due to solar rotation. *Planet and Space Sci* 53:1401–1418
- Withers P, Mendillo M, Hinson DP, Cahoy K (2008) Physical characteristics and occurrence rates of meteoric plasma layers detected in the Martian ionosphere by Mars Global Surveyor Radio Science Experiment. *J Geophys Res* 113:A12314, doi: 10.1029/2008JA013636
- Haider, S.A., and K.K. Mahajan (2014), Lower and upper ionosphere of Mars, *Space Sci. Rev.* Doi:10.1007/s11214-014-0058.2.

12. Pandya BM, Haider SA (2012) Meteor impact perturbation in the lower ionosphere of Mars: MGS observations. *Planet Space Sci* 63/64:105–109, 837–839, doi:10.1126/science1117755
13. Patzold M, Tellmann S, Hausler B, Hinson D, Schaa R, Tyler GL (2005) A sporadic third layer in the ionosphere of Mars. *Science* 310:837–839, doi: 10.1126/science1117755
14. Withers P, Fillingim MO, Lillis RJ, Hausler B, Hinson DP, Tyler GL, Patzold M, Peter K, Tellmann S, Witasse O (2012) Observations of the nightside ionosphere of Mars by Mars Express Radio Science Experiment (MaRs). *J Geophys Res* 117:A12307, doi: 10.1029/2012JA018185
15. Haider SA, Pandya BM, Molina-Cuberos GJ (2013) Nighttime ionosphere caused by meteoroid ablation and solar wind electron-proton-hydrogen impact on Mars: MEX observation and modeling. *J Geophys Res* 118:1–9, doi: 10.1002/jgra.50590
16. Berg OE, Gerloff U (1971) More than two years of micrometeorite data from two Pioneer satellites. *Space Res* 11:225–235
17. Hoffmann H-J, Fechtig H, Grun E, Kissel J (1975) First results of the micrometeoroid experiment S215 on HEOS 2 satellite. *Planet Space Sci* 23:215–224
18. Naumann RJ, DW Jex, CL Johnson (1969) Calibration of Pegasus and Explorer XXIII detector pannels. NASA Tech Rep. TR R-321
19. Grun E, Zook HA, Fechtig H, Giese RH (1985) Collisional balance of the meteoritic complex. *Icarus* 62:244–272
20. Drolshagen G, (2009) Comparison of Meteoroid Models. IADC AI 24.1, Final Report Issue: final; 05-Nov-2009
21. Bauer SJ (1973) *Physics of Planetary Ionospheres*. Springer, New York
22. Bougher SW, McDunn TM, Zoldak KA, Forbes JM (2009) Solar cycle variability of Mars dayside exospheric temperatures; Model evaluation of underlying thermal balance. *Geophys Res Lett* 36:L05201, doi: 10.1029/2008GL036376
23. Jones W (1997) Theoretical and observational determinations of the ionization coefficient of meteors. *Mon Not R Astron Soc* 288:995–1003
24. Helmer H, Plane JMC, Qian J, Gardner CS (1998) A model of meteoric iron in the upper atmosphere. *J Geophys Res* 103:10913–10925
25. Whalley CL, Plane MC (2010) Meteoric ion layers in the Martian 533 atmosphere. *Faraday Discuss* 147:349–368. doi:10.1039/c003726E
26. Whalley CL, Martin JCG, Wright TG, Plane MC (2011) A kinetic 535 study of Mg+ and Mg containing ions reacting with O3, O2, N2, CO2, N2O and 536 H2O: Implications for magnesium ion chemistry in the upper atmosphere. *Phys 537 Chem Chem Phys* 13:6352–6364. doi:10.1039/c0cp02637a
27. McNeil WJ, Lai ST, Murad E (1996) A model for meteoric Magnesium in the ionosphere. *J Geophys Res* 101(A3):5251–5259
28. Pesnell WD, Grebowsky JM (2000) Meteoric magnesium in the Martian atmosphere. *J Geophys Res* 105:1695–1703
29. Pequignot D, Aldrovandi SMV (1986) The ionization balance in HI regions. *Astron Astrophys* 161:169–176
30. Moorhead A, Wiegert PA, Blaauw R, Cook WJ (2014) The meteoroid fluence at Mars due to comet C/2013 A1 (Siding Spring). *Icarus* 231:13–21
31. Tricarico P, Samarasinha NH, Sykes M, Li J-Y, Farnham TL, Kelley MSP (2014) Delivery of dust grains from comet C/2013 A1 (Siding Spring) to Mars. *Astrophys J Lett* 787:L35, doi: 10.1088/2041-8205/787/2/L35
32. Kelley SPM, Farnham TL, Bodewits D (2014) A study of dust and gas at Mars from comet C/2013 A1 (Siding Spring). *Astrophys J Lett* 792:L16, doi: 10.1088/2041-8205/792/1/L16

Submit your manuscript to a SpringerOpen[®] journal and benefit from:

- Convenient online submission
- Rigorous peer review
- Immediate publication on acceptance
- Open access: articles freely available online
- High visibility within the field
- Retaining the copyright to your article

Submit your next manuscript at ► springeropen.com
